Degenerate sequence recognition by the monomeric restriction enzyme: single mutation converts BcnI into a strand-specific nicking endonuclease

Georgij Kostiuk, Giedrius Sasnauskas, Giedre Tamulaitiene and Virginijus Siksnys*

Institute of Biotechnology, Vilnius University, Graiciuno 8, LT 02241, Vilnius, Lithuania

ABSTRACT

Unlike orthodox Type II restriction endonucleases that are homodimers and interact with the palindromic 4–8-bp DNA sequences, BcnI is a monomer which has a single active site but cuts both DNA strands within the 5′-CC↓CGG-3′/3′-GGG↓CC-5′ target site ('↓' designates the cleavage position). Therefore, after cutting the first strand, the BcnI monomer must re-bind to the target site in the opposite orientation; but in this case, it runs into a different central base because of the broken symmetry of the recognition site. Crystal-structure analysis shows that to accept both the C:G and G:C base pairs at the center of its target site, BcnI employs two symmetrically positioned histidines H77 and H219 that presumably change their protonation state depending on the binding mode. We show here that a single mutation of BcnI H77 or H219 residues restricts the cleavage activity of the enzyme to either the 5′-CCCGG-3′ or the 5′-CCGGG-3′ strand, thereby converting BcnI into a strand-specific nicking endonuclease. This is a novel approach for engineering of monomeric restriction enzymes into strand-specific nucleases.

INTRODUCTION

Orthodox Type II restriction endonucleases (REases) are dimers of identical subunits that bind palindromic 4–8 bp DNA sequences and cut both DNA strands to make a double strand break. These enzymes form complexes in which the DNA and the protein share a 2-fold rotational axis of symmetry, placing the catalytic center and sequence recognition elements of one enzyme subunit against the scissile phosphate and DNA bases in one half of the recognition site and the other enzyme subunit against the symmetry related half-site (1,2). In contrast to the orthodox REases, a subgroup of Type II enzymes

including MspI, HinP1I, MvaI and BcnI interact with their recognition sites as monomers, forming asymmetric complexes where the single protein subunit makes contacts to the entire target sequence. Since these enzymes contain only a single active site, it was suggested that they introduce double-strand breaks by sequentially nicking individual DNA strands (3–6). MspI and HinP1I recognize palindromic target sites 5′-C↓CGG-3′ and 5′-G↓CGC-3′ ('↓' marks the cleavage position), respectively (3,7). Due to the 2-fold symmetry of the target sites, MspI and HinP1I encounter the same sequence while binding to the complementary strands. However, this is not true for BcnI and MvaI which interact with the pseudo-palindromic sites 5′-CC↓SGG-3′ (S stands for C or G) and 5′-CC↓WGG-3′ (where W stands for T or A), respectively (5,6). Due to the broken symmetry at the center of their target sites, MvaI and BcnI run into different sequences while switching between the complementary strands. Indeed, to cut both DNA strands within its target site 5′-CC↓SGG-3′, BcnI monomer must be able to interact with both the 5′-CCCGG-3′ and 5′-CCGGG-3′ sequences that differ in the identity of the central nucleotide (Figure 1A, top). In other words, the enzyme must recognize two alternative C:G and G:C orientations of the central base pair but discriminate against other base pairs.

The available crystal structures of BcnI–DNA complex provide atomic details of the central base pair recognition by BcnI. In the first structure (accession code 2ODI), the enzyme is bound to the DNA exclusively in the orientation that brings the C-strand (5′-CC<u>C</u>GG-3′) close to the active site (8). Nearly all H-bond donor and acceptor sites at the central C:G base pair are involved in H-bond interactions with amino acid residues of BcnI. In the minor groove, the enzyme makes a single direct hydrogen bond between N3 atom of guanine and Oδ atom of D32 residue and two water-mediated hydrogen bonds involving the O2 atom of cytosine and the N2 atom of guanine. In the major groove, the Nε atom of H77 forms a hydrogen bond with the N4 atom of cytosine while the Nε atom of H219 forms

---
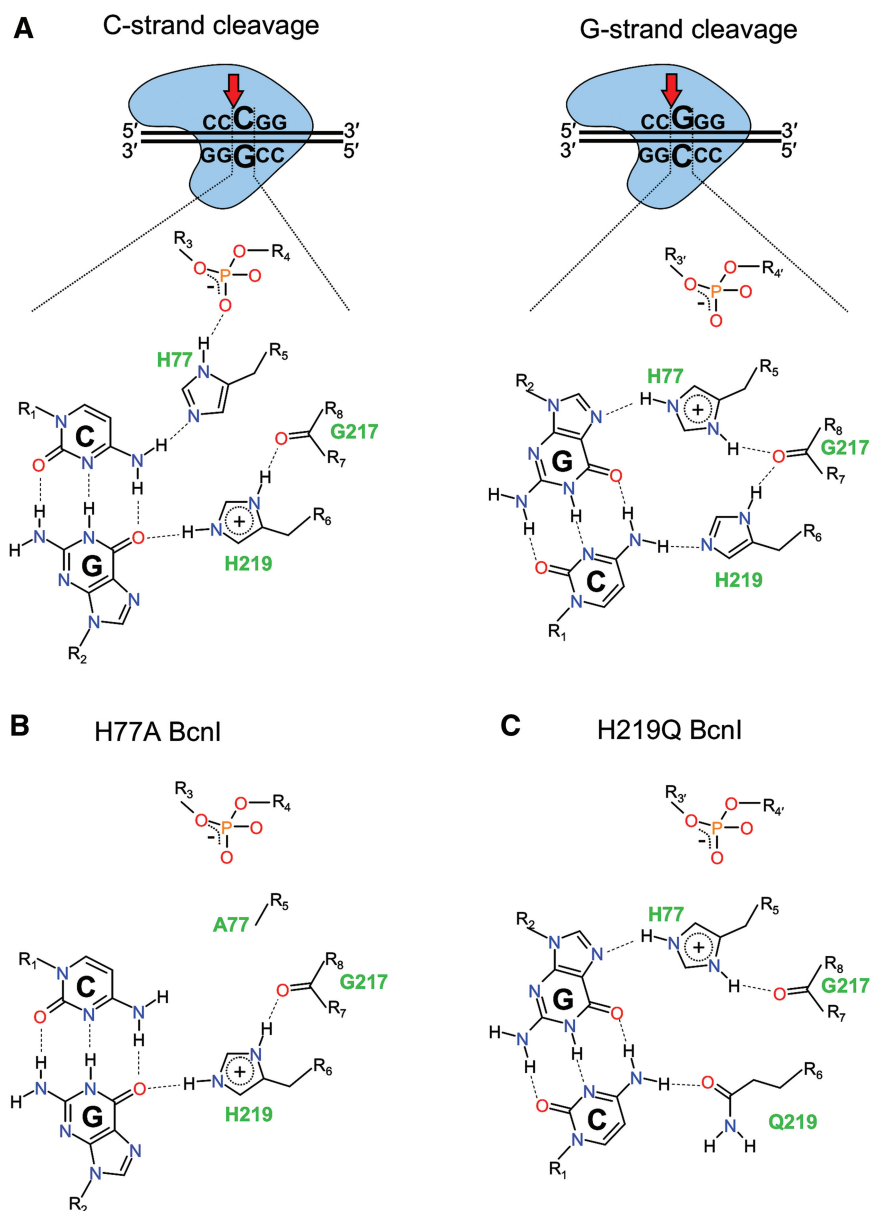
Figure 1. Recognition of the central C:G base pair in the BcnI–DNA complex. (**A**, top) Schematic representation of the wt BcnI interaction with the C-(5′-CCCGG-3′) and G-(5′-CCGGG-3′) DNA strands. The monomeric enzyme with a single active site cleaves individual DNA strands in two separate nicking reactions. (A, bottom) Major groove interactions with the central base pair in two different enzyme orientations: the C-strand close to the catalytic center [PDB accession code 2ODI, (6)] and the G-strand close to the catalytic center (PDB accession code 3IMB). BcnI matches the different pattern of hydrogen bond acceptors and donors in the alternative DNA orientations by switching the protonation state of H219 and H77 residues. (**B**) Possible model for the C:G base pair recognition by the BcnI mutant H77A in the orientation that enables cleavage of the C-strand. (**C**) Possible model for the G:C base pair recognition by the BcnI mutant H219Q in the orientation that enables cleavage of the G-strand.

a hydrogen bond with the O6 atom of guanine (Figure 1A, bottom). As the Nδ atoms of both H77 and H219 are in contact with H-bond acceptors, the assignment implies that H77 is neutral while H219 is in the charged form (8).

In the second structure (accession code 3IMB), BcnI binds to the target site in the alternative orientation, placing the G-strand (5′-CCGGG-3′) instead of the C-strand close to the catalytic center. The change at the center of the target site does not cause significant perturbations in the BcnI structure. The H-bond network to the central base pair in the minor groove is nearly fully conserved in both binding orientations. In the major groove, however, the change in the central base pair brings a proton acceptor (N7 of guanine) close to H77 and a proton donor (N4 of cytosine) close to H219 (8). To accommodate the different pattern of proton donors and acceptors in the alternative binding mode, H219 residue most likely becomes deprotonated, while the heterocyclic ring of H77 rotates by 180° to make a H-bond between its Nε and the N7 atom of the central guanine (Figure 1A, bottom). This change in the H77 side chain conformation replaces the H-bond between its Nδ atom

and oxygen atom of the adjacent DNA phosphate by the H-bond to the main chain oxygen of G217, implying that now the H77 residue is in the protonated form. Taken together, BcnI evolved an elegant way to recognize both the C:G and G:C base pairs at the central position of the recognition site: it employs two symmetrically positioned histidines that may switch their protonation state depending on the orientation of the bound DNA site.

We asked here whether H77 or H219 mutations which introduce asymmetry at the recognition interface of the central base pair could restrict BcnI binding to one particular strand of the target site. By generating and analyzing a set of BcnI mutants, we identified variants that are selectively impaired in cleavage of either the G- or the C-strand. Consequently, by these mutations BcnI was converted into a nicking endonuclease which cuts only the 5′-CC↓CGG-3′ or 5′-CC↓GGG-3′ sequence. This is a novel approach for engineering of site- and strand-specific nicking endonucleases from Type II restriction enzymes.

MATERIALS AND METHODS

Mutagenesis

The H77A, H77N, H219A, H219N, H219Q, H77A + H219N, H77A + H219A and H77N + H219N mutants of BcnI were obtained by modified QuickChange mutagenesis protocol (9). Fifteen cycles of inverse PCR were performed using pBAD24_R.BcnI plasmid (6) as a template, a pair of inverse primers with the designed mutation in the overlapping region, and Pfu DNA polymerase (MBI Fermentas, Vilnius, Lithuania). Following DpnI digestion of the template DNA, the amplified DNA was used for transformation of *Escherichia coli* host by CaCl$_2$ method. Sequencing of the entire gene of each mutant confirmed that only the designed mutation had been introduced.

Protein expression and purification

Wild-type (wt) and mutant forms of BcnI were expressed in *E. coli* and purified to >95% homogeneity as described earlier (6). Concentrations of all BcnI proteins were determined from A_{280} measurements using extinction coefficient of 21430 M^{-1} cm^{-1}.

DNA substrates

All oligodeoxynucleotides used in this study were purchased from Metabion (Martinsried, Germany).

Oligonucleotide duplexes used in the DNA binding and cleavage experiments are listed in Table 1. 5′-termini of strands forming the oligoduplexes CG, TA and NSP were radiolabeled using 'DNA labeling kit' (MBI Fermentas) and [γ–^{33}P]ATP (Hartmann Analytic, Braunschweig, Germany) prior to annealing of the complementary strands in the annealing buffer (33 mM Tris–acetate, pH 7.9 at 25°C and 66 mM potassium acetate). Phage λ and ΦX174 DNA substrates were purchased from MBI Fermentas.

Specific activity and fidelity index

One unit of BcnI activity is defined as the minimum amount of protein required to completely hydrolyze 1 μg of λ DNA in 50 μl reaction mixture in 1 h at 37°C. The specific activity of wt BcnI and mutant proteins was determined by incubating different amounts of protein with 1 μg of phage λ DNA in 50 μl of the Reaction Buffer (33 mM Tris–acetate, pH 7.9 at 25°C, 66 mM potassium acetate and 0.1 mg ml^{-1} BSA) supplemented with 10 mM magnesium acetate. The reactions were incubated for 1 h at 37°C before being quenched by 15 μl of loading dye solution (75 mM EDTA, 0.3% SDS, 0.01% bromphenol blue and 50% glycerol) and loaded onto 1% agarose gel. Fidelity index (FI), defined as the ratio of the maximum enzyme amount showing no star activity to the minimum amount needed for complete digestion at the cognate recognition site, was determined as described in reference (10).

DNA-binding studies

Increasing amounts of protein were mixed with 0.1 nM of ^{33}P-labeled oligoduplex (CG, TA or NSP, Table 1) in the binding buffer (40 mM Tris–acetate, pH 8.3 at 25°C, 5 mM calcium acetate, 0.1 mg ml^{-1} BSA, 10% v/v glycerol) and incubated for 10 min at room temperature. Free DNA and protein–DNA complexes were separated on the non-denaturing 8% polyacrylamide gel (ratio of acrylamide/N,N'-methylenebisacrylamide 29:1) using 40 mM Tris–acetate (pH 8.3) supplemented with 5 mM calcium acetate as the running buffer. Electrophoresis was run at room temperature for 3 h at 6 V/cm. K_D values were calculated as described in reference (11).

Reactions with supercoiled DNA

Reactions on the supercoiled (SC) ΦX174 DNA were conducted at 25°C in the Reaction Buffer mentioned above

Table 1. Oligonucleotide substrates

Oligoduplex	Sequence[a]	Specification
CG	5′-CGCACGACTTCCCGGAAGAGCACGC-3′ 3′-GCGTGCTGAAGGGCCTTCTCGTGCGTTG-5′	A cognate oligoduplex that carries the BcnI recognition site (underlined)
TA	5′-CGCACGACTTCCTGGAAGAGCACGC-3′ 3′-GCGTGCTGAAGGACCTTCTCGTGCGTTG-5′	A miscognate oligoduplex that carries the T:A base pair at the central position of the target site (underlined)
NSP	5′-CGCACGACTTGTCACAAGAGCACGC-3′ 3′-GCGTGCTGAACAGTGTTCTCGTGCGTTG-5′	A nonspecific oligoduplex

[a]Both strands of the CG- and TA-oligoduplexes were radiolabeled at the 5′-termini with ^{33}P.

supplemented with 5 mM magnesium acetate and 5 mM calcium acetate. Calcium ions significantly decreased the DNA hydrolysis rate of BcnI, permitting manual collection of samples. Inhibition most likely is caused by competition of Ca^{2+} with the obligatory cofactor Mg^{2+} for binding at the active site of BcnI. Reaction mixtures typically contained 1 nM SC DNA and 200 nM enzyme. The reactions were initiated by adding magnesium acetate to the mixture of the other components. Aliquots were removed at timed intervals and quenched with loading dye solution [75 mM EDTA, 0.01% bromphenol blue in 50% (v/v) glycerol] and analyzed by electrophoresis through agarose. The SC, open-circular and linear forms of the plasmid were detected and quantified as described in reference (12).

Reactions with oligonucleotide substrates

DNA hydrolysis reactions were performed at 25°C by manually mixing magnesium acetate solution with the preincubated mix of enzyme and radiolabeled oligoduplex (CG or TA, Table 1) in the buffer lacking Mg^{2+} ions. The final composition of the reactions was 4 nM of DNA and 200–400 nM BcnI in the Reaction Buffer supplemented with 10 mM magnesium acetate. Reaction rates with 200 and 400 nM of enzyme were identical (data not shown), suggesting that all of the substrate was bound to enzyme and the observed rates reflect the conversion of the enzyme-bound substrate to products. Alternatively, reactions were performed either in the pH 6.0 buffer (33 mM Mes–KOH, pH 6.0 at 25°C, 66 mM potassium acetate, 10 mM magnesium acetate and 0.1 mg ml^{-1} BSA) or in the pH 9.5 buffer (33 mM glycine–KOH, pH 9.5 at 25°C, 66 mM potassium acetate, 10 mM magnesium acetate and 0.1 mg ml^{-1} BSA). Samples (8 μl) were collected at timed intervals and quenched by mixing with 10 μl of loading dye solution [95% v/v formamide, 25 mM EDTA, 0.01% bromphenol blue]. Fast reactions were carried out by mixing equal volumes (16 μl) of radiolabeled oligonucleotide (8 nM) preincubated with BcnI enzyme (400–800 nM)

and 20 mM magnesium acetate in a Kin-Tek RQF-3 quench-flow device and, after the chosen time delay, quenching with 2.0 M HCl. The recovered samples (~100 μl) were mixed with 50 μl of Neutralization Solution (3.5 M Tris, 3 % SDS) and 70 μl of loading dye solution. Reaction products were separated by denaturing PAGE (20% 29:1 acrylamide/bis-acrylamide with 8 M urea in Tris–borate buffer). Radiolabeled DNA was detected and quantified by phosphorimager (13). The intact DNA strands comprising the DNA substrates CG and TA and their cleavage products are of different length (25 and 28 nt for intact strands, and 12 and 15 nt for the radiolabeled products, respectively) and were completely separated by denaturing electrophoresis. Thus, cleavage of both top and bottom strands of these substrates could be followed in the same experiment.

Data analysis

Non-linear regression used KyPlot 2.0 software (14). Analysis of single-turnover SC DNA cleavage reactions was performed as described in reference (12) and yielded the rate constant k_1 for DNA nicking and rate constant k_2 for the second DNA strand cleavage. Single turnover oligonucleotide cleavage reactions were analysed by fitting single exponentials to the DNA substrate cleavage data.

RESULTS

BcnI mutants

To probe the role of the H77 and H219 residues in the central base pair discrimination by BcnI, we generated mutant BcnI variants in which either the H77 or the H219 (or both) residues were substituted for alanine, asparagine or glutamine (Table 2). Mutation to alanine eliminates H-bonding interactions to the central base in the major grove since all side chain functional groups are removed (Figure 1B). Asparagine or glutamine replacements retain the H-bonding potential but may require

Table 2. Characterization of wt BcnI and mutants

BcnI protein	Activity (%)	Fidelity index	K_D (nM)[a]			SC DNA cleavage[b]		
			CG	TA	NSP	k_1 (s^{-1})	k_2 (s^{-1})	k_1/k_2
wt	100[c]	670	0.5	≥20[d]	≥20[d]	0.033	0.012	2.7
H77A	30	≈1	0.25	25	≥50[d]	0.010	0.0008	12
H77N	15	15	0.3	≥50[d]	≥50[d]	0.0021	0.0004	5
H219N	10	6	0.4	≥50[d]	≥50[d]	0.035	0.0008	44
H219Q	1	≈1	0.6	≥50[d]	≥50[d]	0.064	0.00015	430
H77N + H219N	1	≥70[e]	20	≥50[d]	≥50[d]	0.00035	0.00008	4.6
H77A + H219N	6	3	0.5	≥100[d]	≥100[d]	0.00053	0.00046	1.2

[a]BcnI–DNA complex dissociation constants (K_D) were determined by EMSA in the pH 8.3 buffer supplemented with 5 mM calcium acetate as described in 'Materials and Methods' section.
[b]Rate constants for SC DNA nicking (k_1) and linearization (k_2) were determined under single turnover reaction conditions at 25°C on phage ΦX174 DNA in the pH 7.9 Reaction Buffer supplemented with 5 mM calcium acetate and 5 mM magnesium acetate as described in 'Materials and Methods' section.
[c]Specific activity of the wt BcnI corresponds to 1.7×10^6 U mg^{-1}.
[d]The exact value of dissociation constant could not be determined due to the absence of defined protein–DNA complex. The protein concentration where half of the DNA is converted into the lower mobility species is indicated as a rough estimate of the K_D value.
[e]Non-specific products were not observed even at the highest protein concentration available.

rearrangements at the protein–DNA interface to overcome geometrical or distance constraints for optimal H-bonding (see Figure 1C for one of the possibilities). All mutant proteins were expressed in *E. coli*, however yields of H219A and H77A + H219A mutants were too low to enable further purification. The six other mutants were purified to near homogeneity as judged by SDS–PAGE and subjected for detailed biochemical characterization.

Cleavage activity and specificity

BcnI H77 and H219 residues are involved in direct H-bonding interactions to the central base pair. Substitutions of these residues may therefore significantly affect the cleavage ability and/or specificity of BcnI. First, we determined the cleavage activity of the wt BcnI and mutant variants on phage λ DNA (Table 2). The specific activity of H219Q and H77N + H219N mutants was significantly decreased (Table 2). Other mutations (H77A, H77N, H219N and H77A + H219N) had a less pronounced effect on the BcnI activity. To test whether mutations of the His residues modulate enzyme specificity, we determined the FI for the wt BcnI and mutant proteins. FI is defined as the ratio of the maximum enzyme amount showing no star activity to the minimum amount needed for complete digestion at the cognate recognition sites (10). The FI of BcnI is greater than 500 (Table 2), indicating that the wt enzyme has a very low star activity and falls within the group of REases with an excellent fidelity (10). On the contrary, all H77 and H219 mutants of BcnI are star-prone (FI values < 15). The H77A and H219Q variants are extremely promiscuous since their FI values are ∼1 (Table 2).
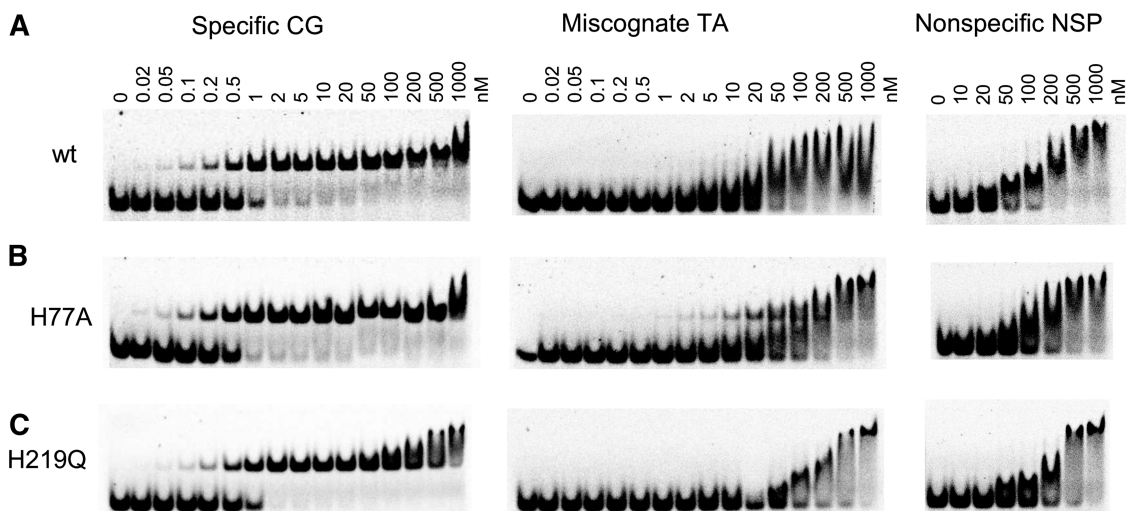
DNA binding

The change in the cleavage activity and promiscuity of BcnI mutants may result from the altered DNA-binding specificity. Therefore, using electrophoretic mobility shift assay (EMSA) we examined BcnI binding to three different substrates (Table 1): the specific CG-oligoduplex bearing the cognate BcnI sequence 5′-CCCGG-3′, the non-specific NSP-oligoduplex lacking the target site and the miscognate TA-oligoduplex that contains the T:A base pair instead of C:G at the center of the BcnI recognition sequence. EMSA studies on this set of oligoduplexes should reveal the ability of wt BcnI and mutant variants to discriminate between the cognate and non-specific sites and between cognate and non-cognate sites that differ only by the base pair at the central position of the recognitions site. The specific DNA-binding affinity for most of the mutants did not change and was similar to the wt BcnI (Figure 2 and Supplementary Figure S1). Only the H77N + H219N mutant binds cognate DNA ∼40-fold weaker than the wt enzyme (Table 2 and Supplementary Figure S1D). Therefore, the decrease in the specific activity for the latter mutant presumably results from the impaired DNA binding. Interestingly, most of the mutations of the His residues responsible for the major groove contacts with the central base pair did not detectably affect the BcnI ability to discriminate between the cognate 5′-CCCGG-3′ and the non-cognate 5′-CCTGG-3′ sequences suggesting the importance of the minor groove contacts in sequence discrimination. The H77A mutant shows preference for the TA- versus the NSP-oligoduplex (Figure 2B), though the binding affinity for the TA-oligoduplex is still ∼100-fold lower in respect to the cognate CG-substrate (Table 2).

Cleavage of SC DNA

The phage λ DNA-cleavage assay monitors reaction products that result from the double-strand breaks at specific sites but does not display reaction intermediates, for example DNA molecules cut at one strand. To detect such reaction intermediates, we analyzed SC phage ΦX174


Figure 2. DNA binding by the wt BcnI and mutants. Electrophoretic mobility shift experiments were performed in the pH 8.3 binding buffer using three different oligoduplexes: the specific CG-oligoduplex, the miscognate TA-oligoduplex and the nonspecific NSP-oligoduplex (Table 1) as described in 'Materials and Methods' section. Protein concentrations used in the experiments are indicated above each lane. (**A**) wt BcnI, (**B**) H77A mutant, (**C**) H219Q mutant. Dissociation constants K_D determined from the electrophoretic mobility shift experiments are provided in Table 2.

DNA cleavage by BcnI and mutant variants under the single-turnover conditions. The ΦX174 circular 5386-bp DNA carries a single 5′-CCSGG-3′ site. Single DNA strand cut should convert the SC substrate into the nicked open circular (OC) intermediate, and cleavage of the second DNA strand should produce the final full length linear (FLL) product (cartoon in Figure 3). Different DNA forms can be separated and quantified using agarose gel electrophoresis (12).

Preliminary experiments revealed that DNA cleavage by BcnI under the single turnover conditions is too fast to be analysed by a manual sample collection (half-life < 4 s). To slow down the reaction, we replaced 10 mM magnesium acetate in the standard reaction buffer by the mixture of 5 mM magnesium acetate and 5 mM calcium acetate. Ca^{2+} ions do not support DNA hydrolysis by BcnI, but presumably compete with the Mg^{2+} cofactor for binding at the active site decreasing the cleavage rate ~200-fold (data not shown). Under these reaction conditions, wt BcnI converts the SC DNA substrate into the final linear product via the nicked OC intermediate (Figure 3A). Such reaction pathway is expected if the monomeric REase cleaves double-stranded DNA in two separate nicking reactions. Fitting the consecutive reaction scheme (cartoon in Figure 3) to the experimental data yielded the reaction rate constants k_1 and k_2 for the cleavage of the first and the second DNA strands, respectively (Figure 3A and Table 2). DNA nicking rate by the wt BcnI is only ~2.5-fold faster than the DNA linearization rate (Table 2) indicating that under the reaction conditions studied enzyme relocation to the second strand after cleavage of the first strand is relatively fast and does not limit the rate of the second strand cleavage. Despite of the 10-fold lower cleavage rate of ΦX174 DNA by H77N, H77A + H219N and H77N + H219N mutants (Table 2), the k_1/k_2 ratio remained similar to wt BcnI (Table 2), suggesting that these mutants, like the wt enzyme, have no preference for a particular DNA strand cleavage. In contrast, H77A, H219N and H219Q mutants acting on ΦX174 DNA predominantly formed the nicked OC intermediate that was further converted into the linear product at a low rate (Figure 3B and C). The k_1/k_2 ratio for the first and the second strand cleavage was approximately 10 for H77A, approximately 40 for H219N and approximately 400 for H219Q (Table 2). The latter three mutants cut one DNA strand much faster than the second strand displaying the phenotype characteristic for nicking endonucleases.

Strand specificity of H77A, H219Q and H219N mutants

Accumulation of the nicked intermediate during SC DNA cleavage by the H77A, H219N and H219Q mutants can be accounted for by two alternative mechanisms: (i) the mutant preferentially binds and cleaves one strand of the target site behaving as a site and strand specific nicking enzyme; (ii) the mutant nicks the target site at either strand but is unable to cut the second strand acting as a site-specific nicking enzyme which has no strand preference.
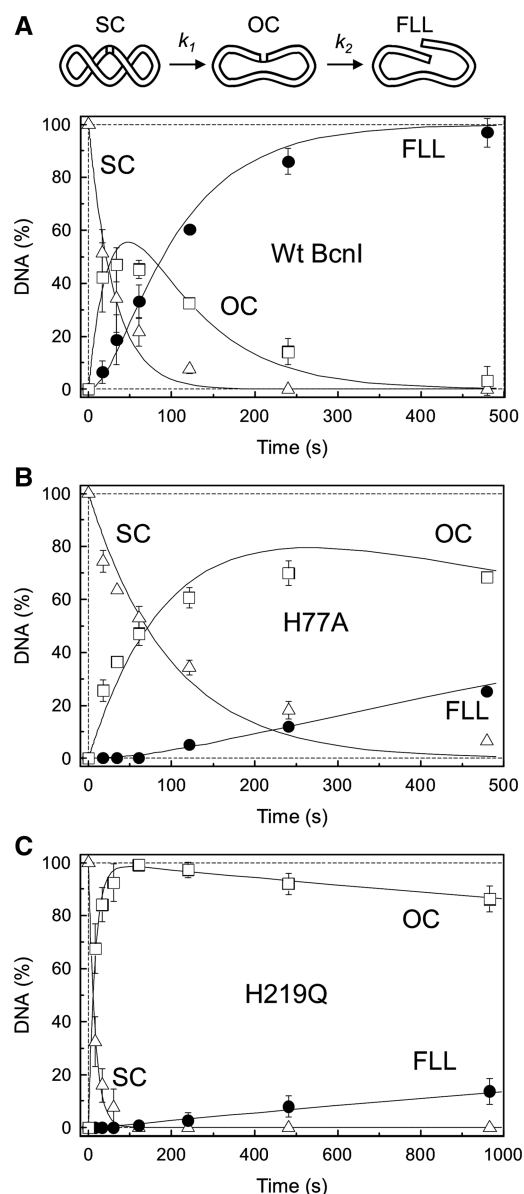
Figure 3. Single-site SC ΦX174 DNA cleavage by the wt BcnI and mutant proteins. The scheme above panel (**A**) illustrates the various DNA forms in the BcnI reaction pathway. Kinetic experiments were performed under single turnover reaction conditions (200 nM enzyme and 1 nM DNA) at 25°C in the pH 7.9 Reaction Buffer supplemented with 5 mM of calcium acetate and 5 mM of magnesium acetate as described in 'Materials and Methods' section. The following DNA forms were separated on agarose gels and quantified: SC DNA, open triangles; nicked OC DNA, open squares; and linear DNA with a double strand break (FLL), filled circles. The proteins were wt BcnI for panel (**A**), H77A mutant for panel (**B**), and H219Q mutant for panel (**C**). The continuous lines in each graph show the best fit to the equations that describe consecutive cleavage of SC substrate into linear product via the nicked intermediate. Determined rate constants for the first reaction step (DNA nicking, rate constant k_1) and the second reaction step (DNA linearization, rate constant k_2) are provided in Table 2.

To determine whether the wt BcnI and mutants exhibit strand specificity, we performed single turnover cleavage experiments using the radiolabeled CG-oligoduplex (Figure 4). Since mutations of H77 and H219 residues
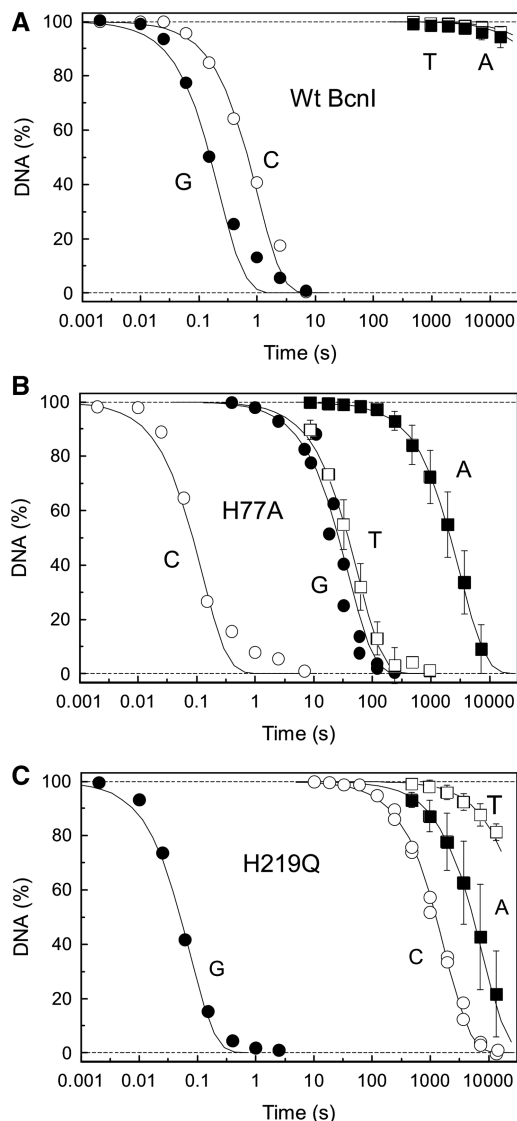
Figure 4. Strand specificity of the wt BcnI and DNA nicking mutants. Kinetic experiments were performed under single turnover reaction conditions (200–400 nM enzyme and 4 nM DNA) at 25°C in the pH 7.9 Reaction Buffer supplemented with 10 mM magnesium acetate as described in 'Materials and Methods' section. The radiolabeled CG- or TA-oligoduplexes (Table 1) were preincubated with enzyme [wt BcnI for (**A**), H77A mutant for (**B**) and H219Q mutant for (**C**)] in the absence of Mg^{2+} ions. DNA cleavage was initiated by addition of magnesium acetate. Hydrolysis of the cognate CG-oligoduplex revealed the cleavage profiles of the C-(5′-CC<u>C</u>GG-3′) and G-(5′-CC<u>G</u>GG-3′) DNA strands (open and filled circles, respectively), while reactions on the miscognate TA-oligoduplex revealed the cleavage profiles of the T-(5′-CC<u>T</u>GG-3′) and A-(5′-CC<u>A</u>GG-3′) DNA strands (open and filled squares). Single exponential fits to the experimental data gave the rate constants $k_{obs}(C)$, $k_{obs}(G)$, $k_{obs}(T)$ and $k_{obs}(A)$ for cleavage of the C-, G-, T- and A-strands, respectively. The rate constants are provided in Table 3.

could relax the specificity of BcnI for the central base pair of the recognition sequence, cleavage rates of individual strands in the TA-oligoduplex were also analyzed (Figure 4). The reactions were performed in the standard reaction buffer supplemented with 10 mM magnesium-acetate; all reactions were initiated by adding Mg^{2+}

solution to the preincubated mixture of enzyme and DNA. Single exponentials were fitted to the cleavage data of every individual strand, resulting in a set of four rate constants [$k_{obs}(C)$, $k_{obs}(G)$, $k_{obs}(T)$ and $k_{obs}(A)$] for the wt BcnI and each of the nicking mutants (Table 3).

BcnI cleaves both C- and G-strands with comparable rates ($k_{obs}(C) \approx 1\,s^{-1}$ and $k_{obs}(G) \approx 4.4\,s^{-1}$, Figure 4A and Table 3), suggesting that the wt enzyme has a moderate preference for the G-strand of the cognate site. Nevertheless, the wt BcnI discriminates extremely well between the cognate 5′-CCSGG-3′ and the miscognate 5′-CCWGG-3′ sites: cleavage rates $k_{obs}(T)$ and $k_{obs}(A)$ of individual strands in the TA-oligoduplex are 10^6-fold slower than in the cognate CG-oligoduplex (Figure 4A and Table 3). The electrophoretic mobilities of 5′-radiolabeled reaction products formed during CG- and TA-oligoduplex cleavage are identical, suggesting that in both substrates cleavage occurred after the second C of the CCNGG sequence (Supplementary Figure S2).

The cleavage pattern of the CG-oligoduplex by the H77A mutant is different. The H77A mutant rapidly cleaves the C-strand [$k_{obs}(C) \approx 8\,s^{-1}$], while cleavage rate of the G-strand is relatively slow [$k_{obs}(G) \approx 0.03\,s^{-1}$, Figure 4B and Table 3] indicating that the H77 replacement to alanine converts BcnI into the strand and sequence specific nicking enzyme albeit with a cost for enzyme specificity. Indeed, cleavage rates of T- and A-strands in the TA-oligoduplex increased by 8000- and 100-fold, respectively, in comparison to the wt BcnI indicating that the ability of H77A mutant to discriminate against the miscognate sequence 5′-CCWGG-3′ is significantly compromised. This is consistent with the EMSA experiments which show enhanced binding of the H77A mutant to the TA-oligoduplex (Figure 2B).

Strikingly, the H219Q mutation converted BcnI into a G-strand specific nicking endonuclease (Figure 4C). Indeed, the cleavage rate differences between the G- and C-strands increased to ~25 000-fold (Table 3). Again, similarly to the H77A mutant, the H219Q mutation compromised the discrimination between the cognate and miscognate sequences (Table 3). The H219N mutant showed similar phenotype but the strand specificity was less pronounced [$k_{obs}(G)/k_{obs}(C)$ ratio ~ 50, Table 3] and the specificity compromised to even higher extent (Table 3). Inspection of the electrophoretic mobilities of DNA hydrolysis products confirmed that all three BcnI mutants retained the cleavage position characteristic for the wt enzyme (Supplementary Figure S2).

DNA recognition by the wt BcnI requires a defined protonation state of the H77 and H219 residues (Figure 1A, bottom). To test whether changes in pH value affect cleavage rates and strand preferences of the wt BcnI and mutant variants, we examined cognate oligoduplex cleavage at pH 6.0 and 9.5 (Supplementary Table S1). Decrease of pH value to 6.0 resulted in severe reduction of reaction rates for all BcnI variants tested; moreover, the strand preferences of H77A and H219Q mutants were significantly diminished. At pH 9.5, wt BcnI and both H219 residue mutants retained their strand preferences and cleaved DNA strands with the

rates comparable to the standard pH 7.9 buffer. In contrast, at pH 9.5 the H77A, mutant lost any preference for the C-strand and cleaved both strands of the cognate substrate at a relatively low rate $[k_{obs}(C) \approx k_{obs}(G) \approx 0.04 \, s^{-1}]$.

DISCUSSION

Type II REases which cut double-stranded DNA at specific sites form an abundant group of enzymes (2,15). In contrast, the number of nicking endonucleases that cleave only one DNA strand at a defined site is much smaller [for a recent review, see ref. (16)]. So far, only a few nicking enzymes (Nt.CviPII, Nt.BstNBI, Nb.BsrDI, Nb.BtsI) were identified in bacteria (17–20) and most of them are the large subunits of the heterodimeric REases (21) (Figure 5A). Since nicking endonucleases are useful molecular tools for DNA amplification, labeling, generation of pre-nicked substrates, etc. (22,23), different approaches for engineering of nicking endonucleases have been developed. Several nicking enzymes have been obtained by inactivation of the catalytic site in one of the subunits in the heterodimeric REases (24,25) (Figure 5B). Alternatively, nicking enzymes were generated by inactivation of one catalytic center in monomeric REases bearing two active sites in one polypeptide chain (21,23,26) (Figure 5C). Furthermore, nicking enzymes were engineered from Type IIS REases

(e.g. AlwI, MlyI, BsaI, BsmBI, BsmAI, SapI, FokI) by various procedures, including site-directed mutagenesis of the dimerization interface, random mutagenesis, domain swapping and reshuffling of protein subunits deficient in DNA recognition and/or cleavage (27–30) (Figure 5D). Under certain reaction conditions, some Type IIS REases preferentially cleave only one DNA strand acting as nicking enzymes (13). In addition, a few nicking enzymes were engineered from homing endonucleases and successfully applied for gene targeting (31,32), thereby expanding the list of naturally occurring nicking homing endonucleases (33,34).

We present here a novel approach to engineering of site and strand-specific nicking endonucleases (Figure 5E). We took an advantage of the fact that Type IIP REase BcnI, specific for the pseudo-palindromic sequence 5′-CCSGG-3′, is a monomeric protein that interacts with the entire recognition site. To generate a double-strand break, BcnI must perform two separate nicking reactions acting consecutively on the C- and G-strands of its recognition site (Figure 1A, top). Analyzing the role of His residues in the central C:G base pair recognition by the BcnI, we have identified two mutant variants (H77A and H219Q) which predominantly form nicked intermediate during the SC DNA cleavage (Figure 3B and C). Using oligonucleotide substrates, we demonstrated that the above mutants are indeed site and strand-specific nicking endonucleases: contrary to the wt BcnI that cleaves both

Table 3. Strand specificity of wt BcnI and mutants

Protein	Cleavage rates[a]				$k_{obs}(G)/k_{obs}(C)$
	$k_{obs}(C)$ (s^{-1})	$k_{obs}(G)$ (s^{-1})	$k_{obs}(T) \times 1000$ (s^{-1})	$k_{obs}(A) \times 1000$ (s^{-1})	
wt BcnI	1.0 ± 0.1	4.4 ± 0.1	0.002 ± 0.001	0.003 ± 0.001	4.4
H77A	8.1 ± 1.0	0.026 ± 0.002	18 ± 2	0.32 ± 0.07	0.0032
H219N	0.109 ± 0.003	5.8 ± 0.3	0.25 ± 0.08	0.045 ± 0.011	53
H219Q	0.00055 ± 0.00005	13.5 ± 1.0	0.018 ± 0.005	0.13 ± 0.04	24500

[a]Rate constants were determined at 25°C in the pH 7.9 Reaction Buffer supplemented with 10 mM magnesium acetate on radiolabeled CG- and TA-oligoduplexes (Table 1) as described in 'Materials and Methods' section. All rate constants are presented as mean values ± 1 SEM.
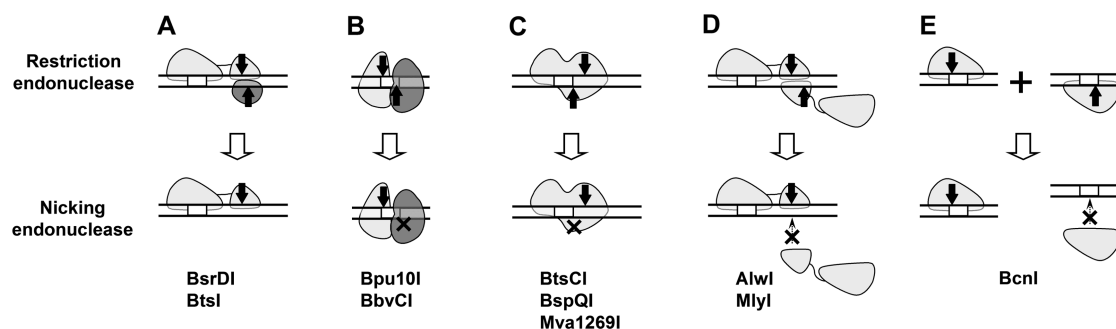
Figure 5. Different approaches towards engineering of REases into strand specific nicking enzymes. DNA strands are shown as two parallel lines, the recognition sequence is boxed. Individual subunits of heterodimeric proteins are colored in different shades of gray. Black arrows mark catalytic centres; '×' marks the catalytically impaired enzyme subunits or reaction stages. (**A**) The large subunit of some heterodimeric Type IIS REase acts as a nicking enzyme in the absence of the small subunit. (**B**) Inactivation of one subunit in the heterodimeric REase selectively blocks cleavage of either the top or the bottom DNA strand. (**C**) Inactivation of one active site in the REase bearing two active sites in a single polypeptide chain yields a nicking enzyme. (**D**) Blocking transient dimerization by mutations at the dimer interface converts some Type IIS REases into nicking enzymes. (**E**) Introducing mutations that restrict the monomeric restriction enzyme binding to particular DNA strand results in the nicking enzyme.

C- and G-strands with comparable rates, the H77A mutant displays a strong preference for the C-strand, while the mutant H219Q prefers the G-strand (Figure 4 and Table 3). Simple calculations using rate constant values provided in Table 3 show that the best nicking variant H219Q in 1 min will completely cut the G-strand but >96% of the opposite C-strand will remain intact. Data for oligoduplex cleavage are consistent with the reaction pattern of the SC ΦX174 DNA cleavage (Supplementary Figure S3).

The observed preference of BcnI mutants for one particular DNA strand is presumably due to the impaired ability of the mutants to bind the pseudo-palindromic target site in both orientations (Figure 1A). Preferential binding of the mutant protein to the target site in one orientation followed by hydrolysis of the phosphodiester bond will result in strand-specific nicking activity. In the preferred orientation, the H77A mutant places the active site close to the C-strand. Comparison of the major groove contacts to the central C:G base pair for the wt enzyme and the H77A mutant (Figure 1) reveals that the alanine replacement should disrupt both hydrogen bonds made by the H77 residue, while the H219 residue should remain positively charged. The loss of the preference for the C-strand by the H77A mutant at pH 9.5 (Supplementary Table S1) may result from the deprotonation of the H219 residue which in the neutral form would be unable to donate a hydrogen bond to the O6 atom of guanine base (Figure 1B) but would still be able to form a hydrogen bond with the N4 atom of the cytosine in the opposite binding orientation. The above model implies that at pH 7.9, where H77A mutant displays a strong preference for the C-strand, the H219 residue should be in the protonated state. Assuming that the pK_a value of imidazole in solution is close to 6.0, the pK_a value of H219 must be perturbed due to the local environment of the protein–DNA interface. However, the observed strand preference of the H77A mutant can not be attributed solely to the protonation state of the H219 residue, as the significant decrease in strand preference is also observed at pH 6.0 (Supplementary Table S1).

The H219Q mutant preferentially places the active site close to the G-strand. According to the model provided in Figure 1C, the H77 is protonated and donates a hydrogen bond to the O6 atom of guanine, while the Q219 forms a hydrogen bond with the N4 atom of the cytosine in the complementary DNA strand. Target sequence binding in the opposite orientation would require deprotonation of H77 and rotation of the side chain of Q219 in order to donate a hydrogen bond to the O6 of guanine. Surprisingly, the H219Q mutant retains the preference for the G-strand (Table 3 and Supplementary Table S1) at all pH values tested (6.0, 7.9 and 9.5) implying that the model may be more complex than initially thought. The crystal structure of the H219Q mutant in complex with cognate DNA would be helpful for our understanding of the strand discrimination mechanism.

Noteworthy, the catalytic center in the nicking variants H77A and H219Q is not compromised: both mutants cleave the preferred strand even faster than the wt enzyme in the standard reaction buffer (Table 3). The dramatic decrease in the specific activity of the nicking mutants on the phage λ DNA (Table 2) is therefore solely due to the slow cleavage of the second DNA strand, as the λ DNA cleavage assay monitors only reaction products that result from the double-strand breaks. The strand preference demonstrated here for the H77A and H219Q mutants comes at a cost of the decreased fidelity since cleavage rate of the non-cognate 5′-CCWGG-3′ sequences is increased (Table 3). Relaxed recognition of the central base pair is consistent with the major groove interactions of H77 and H219 residues (Figure 1 and C): replacement of one of the histidines by smaller alanine or glutamine residues creates more space on the major groove side of the central base pair required to accommodate the T:A bases.

The method for nicking enzyme engineering provided here (Figure 5E) could be applied to other monomeric REases interacting with pseudo-palindromic recognition sequences. The next obvious candidate would be MvaI, an enzyme that recognizes the 5′-CC↓WGG-3′ sequence which is closely related to BcnI (5). Intriguingly, the asymmetric mode of DNA binding and cleavage discovered here for BcnI mutants is observed in the naturally occurring nicking nuclease MutH that shares structural similarities with both BcnI and MvaI (8). MutH, involved in the mismatch repair process in *E. coli*, cleaves the unmodified strand within the hemimethylated sequence 5′-GATC-3′, directing the mismatch-repair process to the unmethylated newly synthesized DNA strand. However, the Y212S mutation enables cleavage of both strands of the hemimethylated substrate by MutH, converting it into a restriction enzyme (35). This demonstrates that engineering of endonucleases can proceed in both ways: a restriction enzyme can be converted into a nicking endonuclease and vice versa.

SUPPLEMENTARY DATA

Supplementary Data are available at NAR Online.

REFERENCES

1. Kelly,T.J. Jr. and Smith,H.O. (1970) A restriction enzyme from *Hemophilus influenzae*. II. *J. Mol. Biol.*, **51**, 393–409.
2. Pingoud,A., Fuxreiter,M., Pingoud,V. and Wende,W. (2005) Type II restriction endonucleases: structure and mechanism. *Cell Mol. Life Sci.*, **62**, 685–707.
3. Xu,Q.S., Kucera,R.B., Roberts,R.J. and Guo,H.C. (2004) An asymmetric complex of restriction endonuclease MspI on its palindromic DNA recognition site. *Structure*, **12**, 1741–1747.
4. Horton,J.R., Zhang,X., Maunus,R., Yang,Z., Wilson,G.G., Roberts,R.J. and Cheng,X. (2006) DNA nicking by HinP1I endonuclease: bending, base flipping and minor groove expansion. *Nucleic Acids Res.*, **34**, 939–948.
5. Kaus-Drobek,M., Czapinska,H., Sokolowska,M., Tamulaitis,G., Szczepanowski,R.H., Urbanke,C., Siksnys,V. and Bochtler,M. (2007) Restriction endonuclease MvaI is a monomer that recognizes its target sequence asymmetrically. *Nucleic Acids Res.*, **35**, 2035–2046.
6. Sokolowska,M., Kaus-Drobek,M., Czapinska,H., Tamulaitis,G., Szczepanowski,R.H., Urbanke,C., Siksnys,V. and Bochtler,M. (2007) Monomeric restriction endonuclease BcnI in the apo form and in an asymmetric complex with target DNA. *J. Mol. Biol.*, **369**, 722–734.
7. Yang,Z., Horton,J.R., Maunus,R., Wilson,G.G., Roberts,R.J. and Cheng,X. (2005) Structure of HinP1I endonuclease reveals a striking similarity to the monomeric restriction enzyme MspI. *Nucleic Acids Res.*, **33**, 1892–1901.
8. Sokolowska,M., Kaus-Drobek,M., Czapinska,H., Tamulaitis,G., Siksnys,V. and Bochtler,M. (2007) Restriction endonucleases that resemble a component of the bacterial DNA repair machinery. *Cell Mol. Life Sci.*, **64**, 2351–2357.
9. Zheng,L., Baumann,U. and Reymond,J.L. (2004) An efficient one-step site-directed and site-saturation mutagenesis protocol. *Nucleic Acids Res.*, **32**, e115.
10. Wei,H., Therrien,C., Blanchard,A., Guan,S. and Zhu,Z. (2008) The Fidelity Index provides a systematic quantitation of star activity of DNA restriction endonucleases. *Nucleic Acids Res.*, **36**, e50.
11. Tamulaitis,G., Mucke,M. and Siksnys,V. (2006) Biochemical and mutational analysis of EcoRII functional domains reveals evolutionary links between restriction enzymes. *FEBS Lett.*, **580**, 1665–1671.
12. Lagunavicius,A., Sasnauskas,G., Halford,S.E. and Siksnys,V. (2003) The metal-independent type IIs restriction enzyme BfiI is a dimer that binds two DNA sites but has only one catalytic centre. *J. Mol. Biol.*, **326**, 1051–1064.
13. Sasnauskas,G., Halford,S.E. and Siksnys,V. (2003) How the BfiI restriction enzyme uses one active site to cut two DNA strands. *Proc. Natl Acad. Sci. USA*, **100**, 6410–6415.
14. Yoshioka,K. (2002) KyPlot – a user-oriented tool for statistical data analysis and visualization. *CompStat.*, **17**, 425–437.
15. Roberts,R.J., Vincze,T., Posfai,J. and Macelis,D. REBASE - a database for DNA restriction and modification: enzymes, genes and genomes. *Nucleic Acids Res.*, **38**, D234–D236.
16. Chan,S.H., Stoddard,B.L. and Xu,S.Y. (2010) Natural and engineered nicking endonucleases - from cleavage mechanism to engineering of strand-specificity. *Nucleic Acids Res.*, Aug 30 (doi: 10.1093/nar/gkq742; Epub ahead of print).
17. Xia,Y.N., Morgan,R., Schildkraut,I. and Van Etten,J.L. (1988) A site-specific single strand endonuclease activity induced by NYs-1 virus infection of a *Chlorella*-like green alga. *Nucleic Acids Res.*, **16**, 9477–9487.
18. Morgan,R.D., Calvet,C., Demeter,M., Agra,R. and Kong,H. (2000) Characterization of the specific DNA nicking activity of restriction endonuclease N.BstNBI. *Biol. Chem.*, **381**, 1123–1125.
19. Xu,S.Y., Zhu,Z., Zhang,P., Chan,S.H., Samuelson,J.C., Xiao,J., Ingalls,D. and Wilson,G.G. (2007) Discovery of natural nicking endonucleases Nb.BsrDI and Nb.BtsI and engineering of top-strand nicking variants from BsrDI and BtsI. *Nucleic Acids Res.*, **35**, 4608–4618.
20. Higgins,L.S., Besnier,C. and Kong,H. (2001) The nicking endonuclease N.BstNBI is closely related to type IIs restriction endonucleases MlyI and PleI. *Nucleic Acids Res.*, **29**, 2492–2501.
21. Zhang,P., Too,P.H., Samuelson,J.C., Chan,S.H., Vincze,T., Doucette,S., Backstrom,S., Potamousis,K.D., Schramm,T.M., Forrest,D. *et al.* (2010) Engineering BspQI nicking enzymes and application of N.BspQI in DNA labeling and production of single-strand DNA. *Protein Expr. Purif.*, **69**, 226–234.
22. Van Ness,J., Van Ness,L.K. and Galas,D.J. (2003) Isothermal reactions for the amplification of oligonucleotides. *Proc. Natl Acad. Sci. USA*, **100**, 4504–4509.
23. Too,P.H., Zhu,Z., Chan,S.H. and Xu,S.Y. (2010) Engineering Nt.BtsCI and Nb.BtsCI nicking enzymes and applications in generating long overhangs. *Nucleic Acids Res.*, **38**, 1294–1303.
24. Janulaitis,A., Stankevicius,K., Lubys,A. and Markauskas,A. (2005), USA Patent No. 6867028.
25. Heiter,D.F., Lunnen,K.D. and Wilson,G.G. (2005) Site-specific DNA-nicking mutants of the heterodimeric restriction endonuclease R.BbvCI. *J. Mol. Biol.*, **348**, 631–640.
26. Armalyte,E., Bujnicki,J.M., Giedriene,J., Gasiunas,G., Kosinski,J. and Lubys,A. (2005) Mva1269I: a monomeric type IIS restriction endonuclease from *Micrococcus varians* with two EcoRI- and FokI-like catalytic domains. *J. Biol. Chem.*, **280**, 41584–41594.
27. Xu,Y., Lunnen,K.D. and Kong,H. (2001) Engineering a nicking endonuclease N.AlwI by domain swapping. *Proc. Natl Acad. Sci. USA*, **98**, 12990–12995.
28. Besnier,C.E. and Kong,H. (2001) Converting MlyI endonuclease into a nicking enzyme by changing its oligomerization state. *EMBO Rep.*, **2**, 782–786.
29. Zhu,Z., Samuelson,J.C., Zhou,J., Dore,A. and Xu,S.Y. (2004) Engineering strand-specific DNA nicking enzymes from the type IIS restriction endonucleases BsaI, BsmBI, and BsmAI. *J. Mol. Biol.*, **337**, 573–583.
30. Sanders,K.L., Catto,L.E., Bellamy,S.R. and Halford,S.E. (2009) Targeting individual subunits of the FokI restriction endonuclease to specific DNA strands. *Nucleic Acids Res.*, **37**, 2105–2115.
31. Niu,Y., Tenney,K., Li,H. and Gimble,F.S. (2008) Engineering variants of the I-SceI homing endonuclease with strand-specific and site-specific DNA-nicking activity. *J. Mol. Biol.*, **382**, 188–202.
32. McConnell,S.A., Takeuchi,R., Pellenz,S., Davis,L., Maizels,N., Monnat,R.J. Jr. and Stoddard,B.L. (2009) Generation of a nicking enzyme that stimulates site-specific gene conversion from the I-AniI LAGLIDADG homing endonuclease. *Proc. Natl Acad. Sci. USA*, **106**, 5099–5104.
33. Landthaler,M. and Shub,D.A. (2003) The nicking homing endonuclease I-BasI is encoded by a group I intron in the DNA polymerase gene of the *Bacillus thuringiensis* phage Bastille. *Nucleic Acids Res.*, **31**, 3071–3077.
34. Shen,B.W., Landthaler,M., Shub,D.A. and Stoddard,B.L. (2004) DNA binding and cleavage by the HNH homing endonuclease I-HmuI. *J. Mol. Biol.*, **342**, 43–56.
35. Friedhoff,P., Thomas,E. and Pingoud,A. (2003) Tyr212: a key residue involved in strand discrimination by the DNA mismatch repair endonuclease MutH. *J. Mol. Biol.*, **325**, 285–297.